Chapter 6
Ion Implantation

G. Langouche and Y. Yoshida

Abstract In this tutorial we describe the basic principles of the ion implantation technique and we demonstrate that emission Mössbauer spectroscopy is an extremely powerful technique to investigate the atomic and electronic configuration around implanted atoms. The physics of dilute atoms in materials, the final lattice sites and their chemical state as well as diffusion phenomena can be studied. We focus on the latest developments of implantation Mössbauer spectroscopy, where three accelerator facilities, i.e., Hahn-Meitner Institute Berlin, ISOLDE-CERN and RIKEN, have intensively been used for materials research in in-beam and on-line Mössbauer experiments immediately after implantation of the nuclear probes.

6.1 Introduction

Among the techniques that can be used to introduce well defined concentrations of impurities into semiconductors, ion implantation turns out to possess particularly attractive properties. It is not dependent on the diffusivity nor the solubility of the dopant atom in the semiconductor host, the substrate does not have to be heated as in a diffusion process, the dosage and the depth distribution of the impurity can be well controlled. On the other hand, in those first years around 1960 when the

G. Langouche (✉)
Department of Physics and Astronomy, University of Leuven, Institute of Nuclear and Radiation Physics, Celestijnenlaan 200D, BE-3001, Leuven, Belgium
e-mail: guido.langouche@kuleuven.be

Y. Yoshida
Shizuoka Institute of Science and Technology, Toyosawa 2200-2, Fukuroi-city, Shizuoka 437-8555, Japan
e-mail: yoshida@ms.sist.ac.jp

Y. Yoshida and G. Langouche (eds.), *Mössbauer Spectroscopy*,
DOI: 10.1007/978-3-642-32220-4_6,

technique became popular, it soon became clear that the atomic configuration of the implanted atom cannot easily be predicted and that the implantation process can lead to extensive damage. Hence room for scientific research on the ion implantation process itself and on the fate of the implanted ion.

Although ion implantation received its main impetus as a technique to dope semiconductors, its use was not limited to this field. When implanting high enough fluencies in semiconductors, it was found that the technique could be used to synthesise conductive layers at well-defined depth inside the semiconductor host, opening a semiconductor technology field of study of its own.

Also ion implantation into metals and insulators was studied. Just as in the case of semiconductors, at low fluencies this allowed to study the atomic configuration around the implanted ion and its defect association. A special field of study was the investigation of the huge internal magnetic fields that implanted atoms were found to experience in magnetic hosts like Fe, Ni and Co. At high fluencies intermetallic surface layers could be formed, and also phenomena like surface hardening and corrosion resistance upon implantation e.g. steel with nitrogen were intensively studied.

This tutorial will not attempt to deal with all these ion implantation phenomena, although Mössbauer spectroscopy has been used in all these fields. We will give several illustrative examples but we will mainly focus on semiconductors and to rather low implantation fluences where the implanted atoms are still isolated from each other or just start to coalesce and to form precipitates. The phenomena at high fluences and the dynamics of compound layer formation are beyond the scope of this tutorial. The reason for this limitation is that emission Mössbauer spectroscopy on radioactive probe atoms is particularly powerful in this low concentration range and allows to study the more fundamental phenomena of lattice location and defect association at the individual probe level, which is hard to study with other techniques. On the other hand, experience has shown that one has to be extremely careful in drawing conclusions from Mössbauer spectroscopy results only, as the possible interpretation of a particular Mössbauer spectrum is often not unique. Complementary data, e.g. from electron microscopy, X-ray diffraction, transport measurements, channelling experiments, are often more than welcome or even crucial for the interpretation of the hyperfine interaction data.

6.1.1 Probing Local Structures and Their Dynamics

Natural science begins with “seeing”. Eyes provide you a first tool to discover wonders of nature. Everyone should have experienced to magnify dragonfly’s eyes and crystals in rocks by loupes, or to watch the surface of the moon and the circle of Saturn by telescope. Nowadays, “electron microscope” and “scanning probe microscope” enable us not only to “see” atoms and their arrangements in materials, but also to manipulate them, in order to create new functional materials and biomaterials. Modern “nanoscience” and “nanotechnology” began with the

discoveries of these "seeing" technologies, which made it possible for us to perform the intensive research work to realize "single electron transistor", "solar cells with an energy conversion efficiency of higher than 40 %", and "Giant Magneto Resistive (GMR)" and "Tunneling Magneto Resistive (TMR)" sensors to produce Terabyte hard disks and a precise positioning encoder on an atomistic scale [1]. When one starts investigating nature on an atomistic scale, such methodologies lead to create new research fields beyond the old frame of science and technology, such as physics, chemistry, biology, electronics, and mechanics.

The microscopes mentioned above allow to observe atoms on the surface and in thin film with a typical thickness of several 10 nm [2]. But how can we investigate the interior of a material on an atomistic scale without destroying the material? Electric resistivity and magnetic susceptibility provide us information on the characteristics of bulk materials. One would like to distinguish, however, the electric and magnetic state of each atom of which the material consists, the crystal structures, as well as their micro- or even nanostructures. X-ray, electron, and neutron scattering methods are, for this purpose, further combined to obtain such structures, i.e. the atomic arrangements in the material. These methods are based on the interference of waves, such as electromagnetic radiation, electron and neutron "waves" [3]. These methods, however, will have more difficulties to observe "the images of the structure", when the micro- and nano-structures tend to possess a unit of structure of the order of nanometers, because the number of atoms inside the structure becomes too small to produce enough intensity of the interference pattern. Is there any other method to "probe" such small structure?

After the discovery of the Mössbauer effect in 1958 by Rudolf Mössbauer [4–6], an atomic nucleus became such a scientific probe, which opens to study the interior of materials through the study of the "hyperfine interaction", which is the interaction between the nucleus and its surrounding electrons [7]. The energy levels of the nucleus are determined by the hyperfine interaction, causing a shift or a splitting of the nuclear energy levels. This level structure can be observed in a Mössbauer spectrum, as has been explained in the former tutorials. The Mössbauer spectrum can be detected via signals such as γ-rays and/or electrons emitted from the nucleus. These signals bring us information on the electric and magnetic states of the probe atom from the interior of the materials, as is schematically shown in Fig. 6.1. The situation can be compared to a "spy", the nuclear probe, who sends a code signal to deliver us secret information from inside the material.

The probe atoms can be one of the constituents of the material, or they can be impurities introduced into the material from the outside by melting, by diffusion, or by implantation. The former processes make use of the thermal motion of the atoms, while the implantation process injects energetic probe atoms using an accelerator. In this tutorial we will further discuss "implantation Mössbauer Spectroscopy", i.e., the probe atoms will be first implanted into a material, and subsequently Mössbauer spectra will be measured by detecting emitted γ-rays and electrons. The spectra will provide us with atomistic information on the probe atoms through the hyperfine interactions. This situation may be well compared with an analogy of a "spy" which is sent to a place to gather information, and he/she will

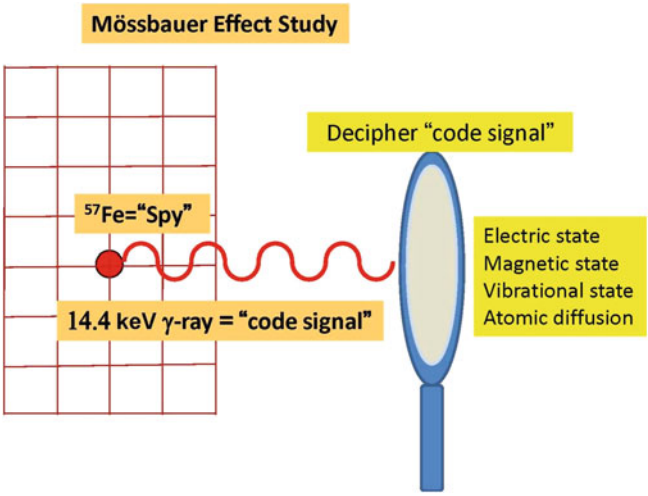

Fig. 6.1 The Mössbauer probe is emitting γ-rays, i.e., a "code signal", which can be deciphered, delivering information on the state of the "spy" in the material

then transmit a code signal to us from this place without disturbing the surroundings. In our case, the code signals are γ-rays and electrons which contain the secret information about the material. The recoil-free γ-ray emission, i.e., Mössbauer effect, will not cause any disturbance at the probe site nor in the surrounding lattice.

6.1.2 Ion Implanters

In this tutorial we will deal with different types of ion implanters. We will first discuss the ion implantation experiments at dedicated "conventional" facilities, meaning that they are of the same type as the ones used in semiconductor industry, but dedicated to the use of radioactive ions. Typical implantation energies in such facilities are in the 50–500 keV range. Figure 6.2 shows a typical ion implanter set-up. It consists of an ion source which usually produces positive ions which are then extracted from this ion source and (pre-)accelerated with a negative voltage of typically about 50–100 kV. This ion beam is then fed into a curved magnet which allows to mass-separate the desired isotope. In the final stage the isotope can still be post-accelerated to a few 100 kV, if desired, and the final stage usually contains magnetic quadrupole lenses to focus the beam and electrodes that allow sweeping the beam over the desired implantation area.

The main difference between a dedicated set-up for hyperfine interaction studies with radioactive probe atoms and a conventional ion implantation set-up is that the dedicated facility is equipped for the handling of radioactive isotopes. As well the ion source stage as the implantation stage need special radioprotection

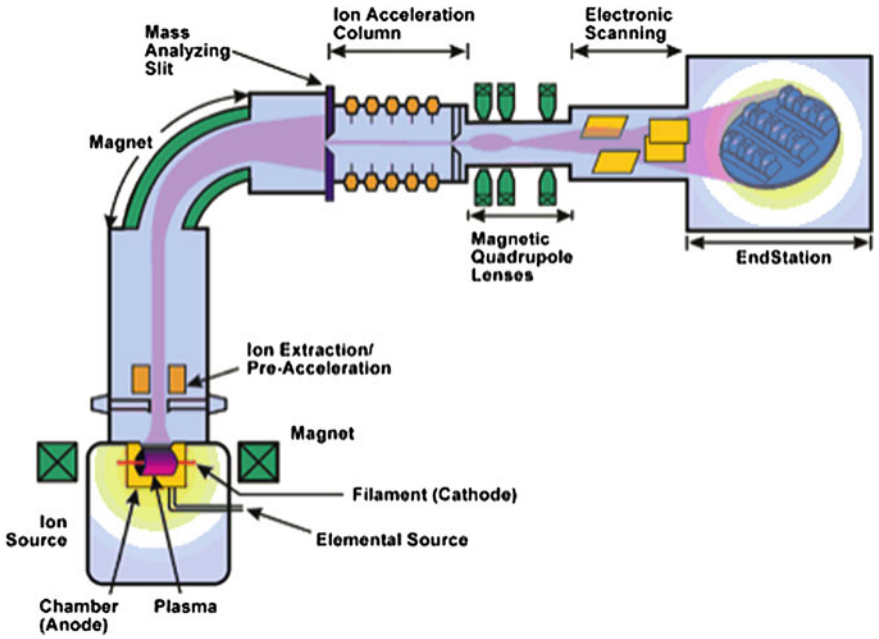

Fig. 6.2 Conventional ion implanter

measures. The inside of the magnet can be covered with a removable lining, which catches the possible radioactive products that are not following the path selected by the magnet setting for the desired isotope. A few laboratories, e.g. at the universities of Groningen, Bonn and Leuven acquired in the 1960s such dedicated experimental facilities to implant relatively long-lived radioactive isotopes. In order to keep the accumulation of radiation in the facility below reasonable limits, the use of radioactive isotopes is these set-ups is normally limited to isotopes with half-lives below one year.

6.1.3 KeV Ion Penetration in Matter

Since the binding energy of atoms in solids is of the order of electron volt, it can be readily expected that ions penetrating in matter with KeV kinetic energy displace many atoms. The phenomena accompanying ions penetrating in matter have been studied in great detail and are well understood. Theoretical treatments can be found in several handbooks [8] and computer codes are available [9] that accurately calculate the implantation profile of particular ions of well-defined energy in solids. Such a profile is characterized by a certain average implantation depth and a certain profile width, called straggling, as shown in Fig. 6.3.

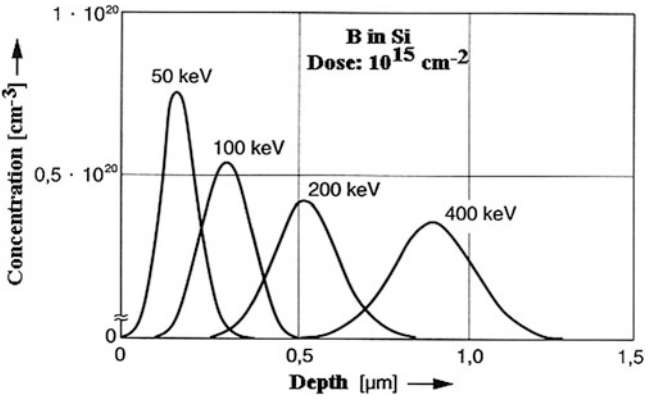

Fig. 6.3 Typical ion implantation profiles

Implantation profiles are the result of many individual penetration paths. Higher energy ions penetrating matter are found to travel first along fairly straight paths, since they are slowed down in this energy range by electronic stopping power, kicking out electrons along their path. Only when slowed down to energies in the tens of KeV range, nuclear collisions start to contribute to the slowing down process, kicking out atoms from their lattice sites and causing the implanted ion to undergo large angle deflection from its original path. These stopping power ranges are illustrated in Fig. 6.4.

Displaced atoms in turn cause damage along their path, so that before finally being stopped in the solid a so-called collision cascade is generated, as shown in Fig. 6.5.

Damage recovery is what happens next. Many displaced atoms finally land up on a regular lattice site again, while others can give rise to permanent defects in the solid. A large variation of possible defect configurations is possible, some of which are more stable than others. The stability of many such defect configurations has been calculated by theorists. The lattice temperature plays a crucial role in the final survival rate of defects and annealing out of defects is a well known procedure after ion implantation in semiconductor industry. Care has to be taken that raising

Fig. 6.4 Stopping power

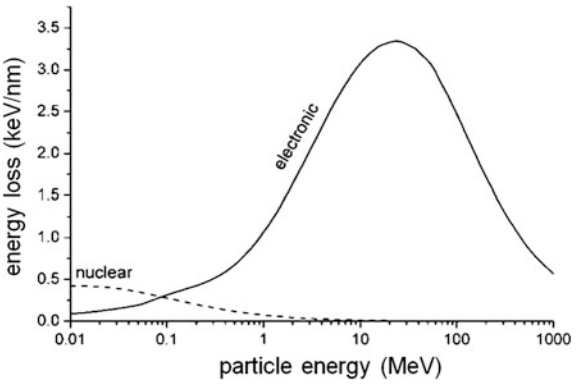

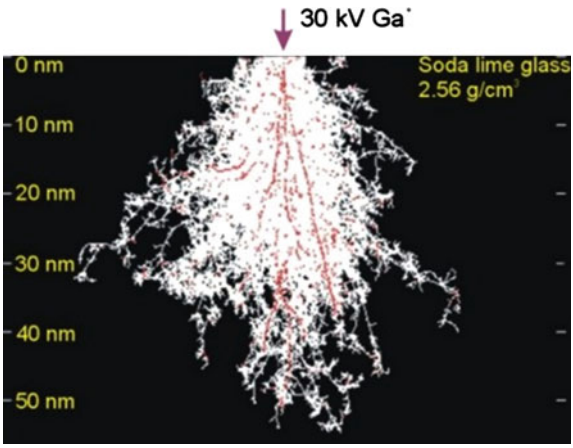

Fig. 6.5 Collision cascade

the temperature does not give rise to unwanted diffusion phenomena in the solid. Special annealing tricks such as flash annealing and laser annealing are sometimes used to avoid such unwanted diffusion phenomena.

Implantation damage is known to anneal out completely in metals even below room temperature. Only implantation at very low temperature where vacancies are not mobile results in observable damage. Except for special cases where chemical affinity plays a role or where e.g. oversized atoms are implanted, ion implantation in metals results in a final so-called replacement collision which results in a substitutional lattice location of implanted atoms.

For semiconductors the story is quite different. Many defects created in the collision cascade are not mobile which can result in defect configurations that do not anneal at room temperature. Heating to higher temperatures is often necessary to anneal out most damage. But it is not unlikely that the implanted atom or part of them remains part of a defect structure. Figure 6.6 illustrates defect recovery after implantation and annealing a semiconductor host.

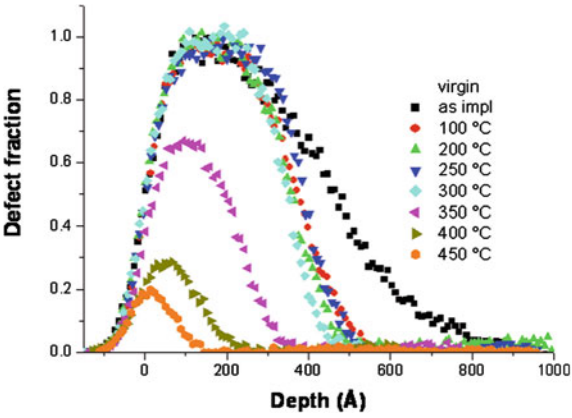

Fig. 6.6 Defect recovery upon annealing

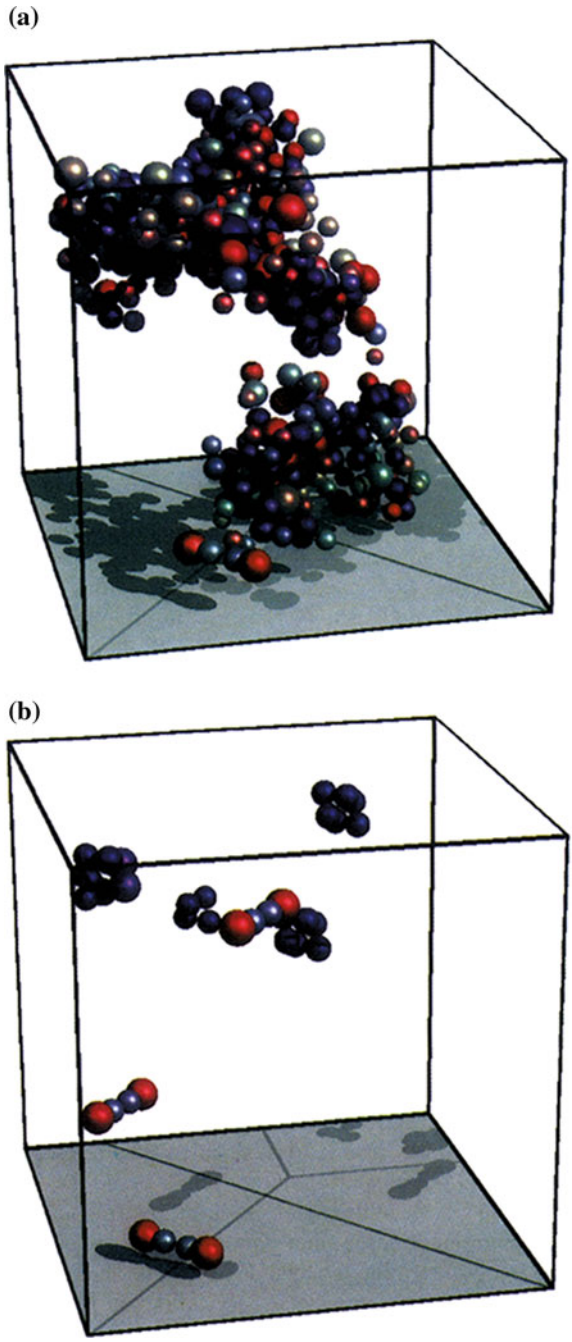

Fig. 6.7 Annealing of cascade-induced amorphous pockets by molecular dynamics. **a** State immediately after the cascade. **b** After 1ns annealing at 1300K the amorphous material has recrystallized and self-interstitials and vacancy clusters are left behind. The vacancies and their clusters induce tensile stress in the neighboring atoms and these are shown as blue spheres. The self-interstitials are shown as red and gray spheres [48]

The term "heat spike" has been used to describe the dense mixture of atoms and defects in motion in the core volume (Fig. 6.7) of a collision cascade. Electron microscopy pictures suggests that a heat spike in a semiconductor can lead to the creation of small amorphous zones in semiconductors associated with individual implanted atoms. There is certainly ample evidence that the accumulation of implantation defects can lead to the creation of amorphous layers inside the semiconductor. Implantation at higher temperature can avoid the creation of such amorphous layers and is more effective than post-implantation annealing at this temperature after an amorphous layer has been formed.

6.1.4 Hyperfine Interactions

Hyperfine interaction techniques with implanted radioactive probe atoms turned out to offer a wealth of information to study the atomic configuration and possible defect association of implanted probe atoms. Several hyperfine interaction techniques, e.g. Mössbauer Spectroscopy, Perturbed Angular Correlations, Low Temperature Nuclear Orientation, Muon Spin Rotation, and Beta-NMR are making use of implanted radioactive probe atoms. We refer to the proceedings of the Hyperfine Interaction Conferences, held every two or three years, for reports on many of these studies. Except for the earliest conferences, all these proceedings were published in the journal Hyperfine Interactions.

It is well known to the Mössbauer Spectroscopy community that Mössbauer probes can be studied in absorption spectroscopy, where the Mössbauer probe under investigation is present in its stable ground state, and in emission spectroscopy, where the Mössbauer probe under investigation is formed in the decay of a radioactive parent nucleus. By far the majority of Mössbauer studies are in absorption spectroscopy. Despite the fact that emission spectroscopy studies are more cumbersome since they require the handling of radioactive parent atoms, they have the interesting property that low concentrations of probe atoms can be studied. A very large fraction of Mössbauer ion implantation studies are such emission spectroscopy radioactive probe studies. A large fraction, indeed, but not all: in a few interesting experiments both absorption and emission Mössbauer spectroscopy was used to study the behaviour of some implanted elements in solids. This tutorial focuses on the use of emission Mössbauer spectroscopy to study ion implanted systems.

The largest part of the emission Mössbauer spectroscopy work is devoted to semiconductors since lattice location and defect association are particularly important there and relevant for semiconductor industry. For a more general picture of hyperfine interactions in semiconductors, also including non-nuclear techniques we refer to [10]. An overview of Mössbauer studies on semiconductors, also including diffusion studies and studies where Mössbauer atoms are constituent atoms of the semiconductor matrix (e.g. ZnTe) can be found in [11]. Already in the 1960s implantation studies [12, 13] were performed with radioactive probe atoms

and studied using Mössbauer Spectroscopy. The early emission Mössbauer spectroscopy implantation work has been discussed in several review articles [14–17].

In the preceding paragraphs we have described a dedicated conventional ion implantation facility, using fairly long-lived activity so that there is enough time to transport the radioactive source from the ion implanter to a Mössbauer spectrometer for what is generally called *off-line experiments*. A somewhat confusing name maybe in cases where the Mössbauer spectrometer is connected to the implanter in order e.g. not to break the vacuum or to raise the temperature, as described in the Sect. 6.2. The term *on-line* emission Mössbauer experiment is reserved for facilities where the radioactive lifetime of the parent isotope is so short that measurements have to be done in situ. The ISOLDE facility at CERN and the RIKEN facility in Tokyo are such facilities, and are described in Sects. 6.4 and 6.5 respectively. A special type of on-line facilities are those facilities where the production, implantation and Mössbauer measurement occur on the time scale of the lifetime of the involved nuclear Mössbauer state, typically shorter than 10^{-6} s. Implantation generally occurs through the recoil of a Coulomb excited atom. Such experiments are generally called *in-beam* Mössbauer experiments experiments and Sect. 6.3 is devoted to ^{57m}Fe in-beam Mössbauer experiments at such a facility at the Hahn-Meitner Institute in Berlin.

In short, the three different types of emission Mössbauer spectroscopy are distinguished by the lifetime of the parent atom. For the Mössbauer isotope ^{57}Fe these parents are:

- off-line experiments use the ^{57}Co parent with $T_{1/2} = 270$ d
- on-line experiments use the ^{57}Mn parent with $T_{1/2} = 1.5$ min
- in-beam experiments use the ^{57m}Fe parent with $T_{1/2} = 10^{-6}$ s

6.2 Off-line ^{57}Co/^{57}Fe Implantation Mössbauer Studies at the Leuven Ion Implanter

The Ion and Molecular Beam Laboratory at the Institute for Nuclear and Radiation Physics at the University of Leuven has a dedicated conventional ion implanter, as defined in the previous paragraph. Nowadays it is part of a network of coupled facilities, as shown in Fig. 6.8, allowing to move samples from one facility to another, without breaking the vacuum.

The UHV system shown in Fig. 6.8 has different analysis and preparation devices (including two Molecular Beam Epitaxy systems) among which also a facility for Conversion Electron Mössbauer Spectroscopy measurements. It is the lead-wrapped facility on the right of Fig. 6.9. The tube in the middle of Fig. 6.9 is an ultra high vacuum transport tube that can be used to transport samples from one facility to another. The facility on the front left of Fig. 6.9 is a MBE-system. It contains a Knudsen cell allowing to evaporate ^{57}Fe onto surfaces. Other layers can be evaporated on top of this layer so that samples can be prepared for ^{57}Fe Mössbauer studies at surfaces and interfaces.

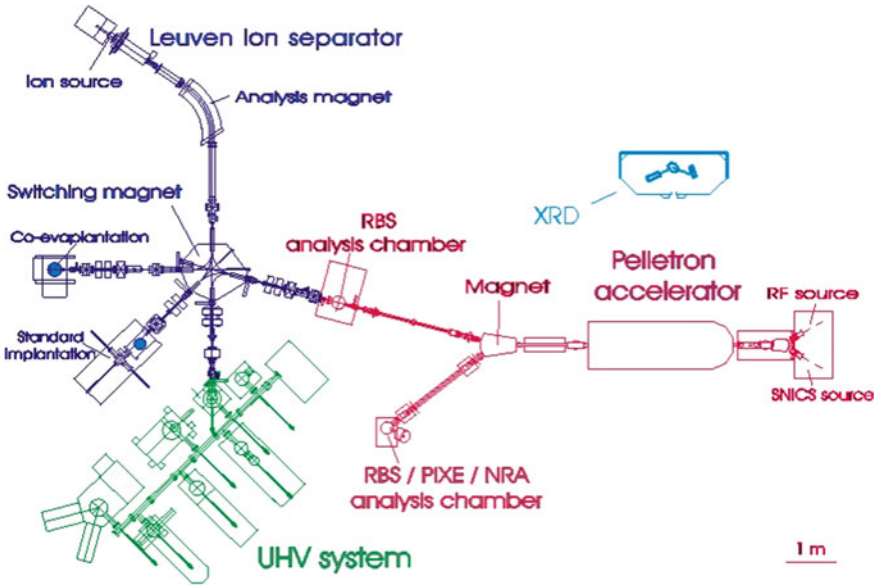

Fig. 6.8 Leuven Ion and Molecular Beam Laboratory

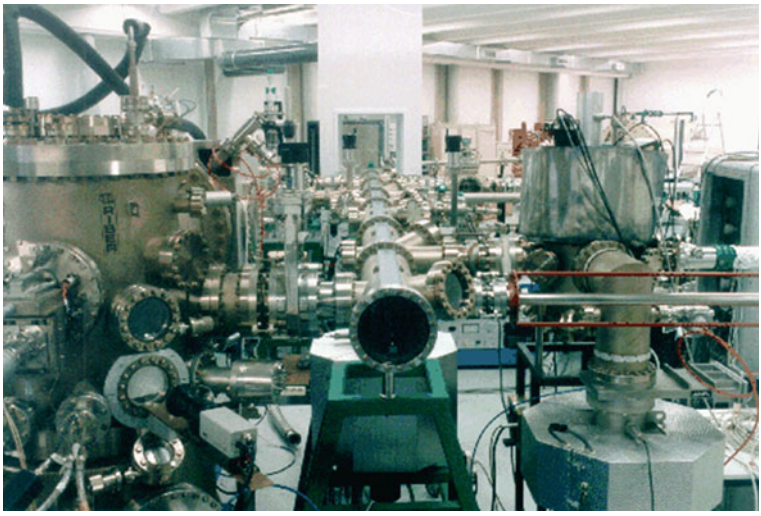

Fig. 6.9 Detailed view of the UHV system of Fig. 6.8

The Pelletron accelerator at the right of the layout shown of Fig. 6.8 is mainly meant to produce 2 MeV He particles for Rutherford Backscattering Spectroscopy studies. Such studies [8] allow a depth selective analysis of the composition of a sample. In channelling geometry it can also be used to determine, with

subnanometer precision, the site location of impurity atoms in a single crystal lattice. The minimum impurity concentration needed for such studies is substantially higher than what can be studied in Mössbauer spectroscopy experiments.

Fe in Si shows a complex behaviour which has challenged Mössbauer physicists for almost 50 years and even today still is not fully understood. As will be discussed in Sect. 6.5 of this chapter, it is still a challenge for semiconductor industry.

In a review paper on "The Mössbauer search for Fe in Si" it is stated [18] that among the close to one thousand papers that so far had been published on Mössbauer spectroscopy studies in semiconductors, involving twenty different elements, the Mössbauer work on ^{57}Fe work in Si had been particularly combersome. In early Mössbauer experiments, as early as 1962 [19, 20], shortly after the discovery of the Mössbauer effect in 1958, the role of precipitate formation during diffusion was insufficiently realized, and the interpretation of the data was not very reliable. After ion implantation the Mössbauer spectra of ^{57}Fe in Si, both in emission Mössbauer spectroscopy, after implanting radioactive ^{57}Co [21], as in absorption Mössbauer spectroscopy, after implanting ^{57}Fe [22], were dominated by two single lines. Also in early in-beam experiments by the Stanford group, starting from the ^{57m}Fe parent state, a technique discussed in Sect. 6.3, two lines were observed [13, 23] with asymmetric intensities.

A controversy arose about the interpretation of these two lines. As can be seen in Fig. 6.10, in ^{57}Co/^{57}Fe emission experiments the line intensities varied as a function of implantation fluence. In ^{57}Fe(Si) absorber experiments, after implantation at fluences higher than to the highest fluences used in Fig. 6.10, a fairly symmetric doublet was observed. In the in-beam Mössbauer experiments, at implantation fluences lower than the lowest fluences shown in Fig. 6.10, an asymmetric doublet was observed. Was there a common interpretation possible?

It was thought that the two single lines might be representative of two implantation sites, presumed to be substitutional and interstitial Fe in Si, but the observed dose dependence could not be accounted for. By applying an external magnetic field it could unambiguously be shown [24] that the high fluence ^{57}Fe(Si) spectrum was a quadrupole interaction doublet, with parameters very similar to those of amorphous Fe_xSi_{1-x} films [22] and hence associated with Fe atoms in an amorphized surrounding.

The origin of the asymmetry at lower fluencies was first accounted for by new emission Mössbauer experiments whereby ^{57}Co was implanted into Si held at the temperature of 50 K [25]. This cold implantation completely reversed the asymmetry (Fig. 6.11) in the spectrum compared to room temperature implanted samples. The model put forward was that at low temperatures, where vacancies are not mobile, ^{57}Co/^{57}Fe atoms land up in interstitial sites in Si, a site preferred by transition metals in Si. Upon increasing the temperature to room temperature, vacancies become mobile at about 100 K and are trapped by the interstitial Co atoms that become substitutional.

New experiments on Fe in Si with the in-beam Mössbauer spectroscopy technique were performed at the Hahn-Meitner institute in Berlin. The technique is outlined in Sect. 6.3. The results of these Coulomb excitation recoil implantation studies [26] confirmed this picture and led to an unambiguous identification of

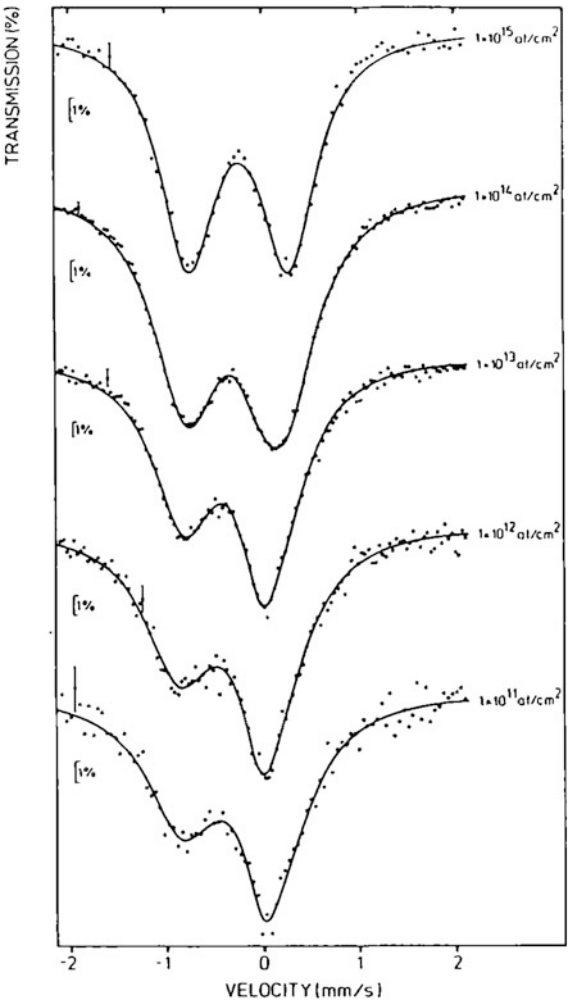

Fig. 6.10 $^{57}Co/^{57}Fe$ Mössbauer spectra as a function of ion implantation fluence [21]

interstitial Fe in Si. The spectra, shown in Fig. 6.12, were interpreted as composed of the "amorphous" doublet and a superimposed single line (with isomer shift $\delta = +\ 0.84(1)$ mm/s with respect to α-Fe).

Due to the improved statistics, an increase in the linewidth of this single line could be observed for higher target temperatures. This line broadening was analyzed in terms of a diffusional motion of the iron atoms, which are able to make atomic jumps within the lifetime of the excited nuclear state. Diffusion coefficients were derived (Fig. 6.13) from the broadening of the Mössbauer lines, and these were found to be remarkably consistent with the known high- and low-temperature diffusion coefficients of Fe in Si.

For the "amorphous" site (isomer shift $\delta = +\ 0.20(3)$ mm/s, quadrupole splitting $\Delta = 0.95(5)$ mm/s) no microscopic model exists up to today. It is dominant in

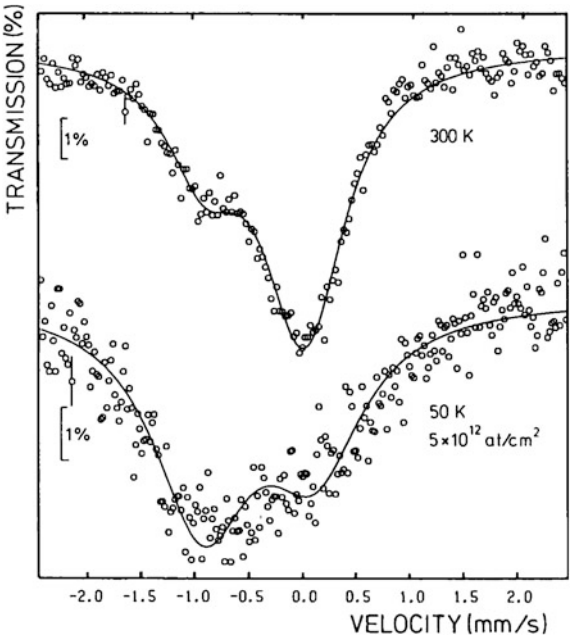

Fig. 6.11 ^{57}Fe spectra after ion implantation of ^{57}Co at 50 K and after subsequent annealing [25]

high fluence implantation experiments, as well as in Fe_xSi_{1-x} films for low x values, and appears to contribute also to the spectra at low fluence. This defect configuration is therefore often called the "amorphous site" and thought to be representative of the amorphized region generated by the collision cascade of single implanted ions.

A substitutional configuration was suggested for a third site ($\delta = -0.07(3)$ mm/s) on the basis of the $Fe_i + V \rightarrow Fe_s$ model and from theoretical calculations. This configuration is attributed to Fe atoms that find themselves outside the amorphized collision cascade region, or in a recrystallized part of it.

Upon annealing low fluence implanted ^{57}Co/^{57}Fe a surprising observation was made. A new spectrum component appeared (Fig. 6.14) with extra Mössbauer resonances at both sides of the spectrum components discussed so far.

It would lead us so far to discuss in detail the dependence of this spectrum component on annealing temperature, fluence and substrate doping. Based on these dependencies, it has been assigned to Co_2 pairs in Si [27].

Also other pairs were recognized, formed by normal acceptors in Si and Co donor atoms (CoB, CoAl, CoGa, CoIn) [28]. The different Fe and Co silicides have been characterized in several experimental studies and are observed as small precipitates after diffusion experiments and also in larger (often epitaxial) structures in ion beam mixing experiments, or in experiments to form buried epitaxial layers. A discussion on studies on these larger configurations around Fe in Si is beyond the scope of this tutorial.

We will also not discuss other Mössbauer probes in semiconductors, e.g. the 5sp-elements ^{119}Sn, ^{121}Sb, ^{125}Te and ^{129}I. They were used with success to probe

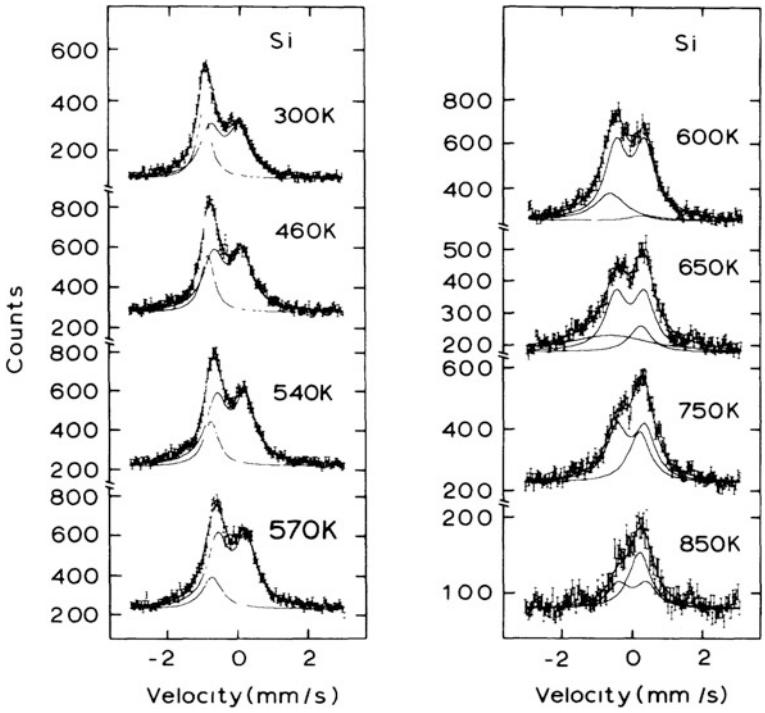

Fig. 6.12 ^{57}Fe spectra after in beam ion implantation of ^{57m}Fe at 50 K and after subsequent annealing [26]

lattice sites and defect configurations after implantation. They offered substantially less difficulties in terms of interpretation compared to Fe in Si. The difference in the chemical nature of these elements is responsible for this less-complicated behavior. On one hand we have the transition metals with their extremely small solubility and extremely high diffusion coefficient in Si, and on the other hand we have an element like Sn, isoelectronic and isostructural with the other group IV semiconductor constituents, and the neighboring elements that can replace host atoms in III-V and II-VI semiconductors, or act as natural substitutional donors or acceptors in these semiconductors.

6.3 In-beam ^{57m}Fe Implantation Mössbauer Studies at the Hahn-Meitner Institute in Berlin

6.3.1 In-beam Mössbauer Spectroscopy Technique

The Stanford group was the first to perform in-beam Mössbauer experiments on ^{57}Fe. The principle of the experiment is to excite stable ^{57}Fe atoms from their ground

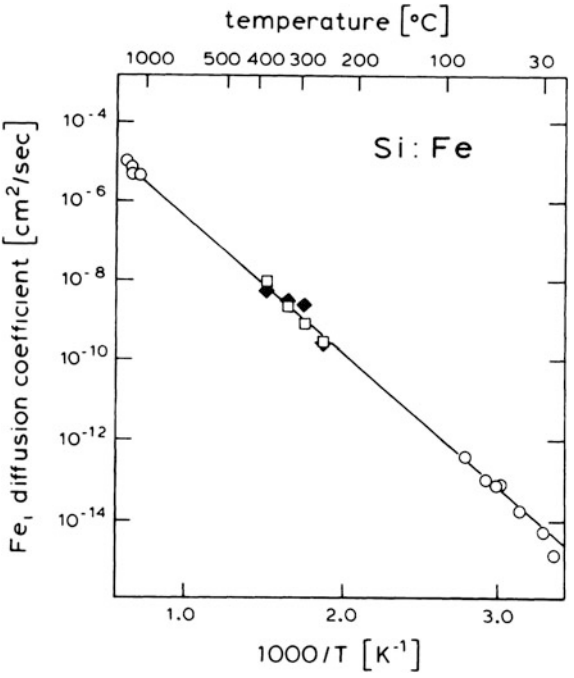

Fig. 6.13 Diffusion coefficients of Fe in Si from the Mössbauer data (*filled squares*) and from other techniques [26]

state into a metastable excited state ^{57m}Fe by the Coulomb interaction between a projectile charged particle and ^{57}Fe nucleus. Subsequently, the excited state ^{57m}Fe decays again to its stable ground state within a lifetime $T_{1/2} = 10^{-6}$ s. The ion implantation and Mössbauer experiment have to be performed within this timespan. If the bombarding energy of such particles is carefully selected to be below the Coulomb barrier, other radioactive nuclei will not be produced, which might otherwise cause a high background for the Mössbauer experiments. As mentioned in the previous section Latshaw [13, 23] applied this technique on Fe in Si.

The technique was further optimized in an experimental set-up at the Hahn-Meitner Institute in Berlin. A sketch of the set-up is shown in Fig. 6.15 [29]. A pulsed beam of 110 MeV ^{40}Ar ions (pulse length $\sim$1 ns, repetition rate $\sim$ 2.5 MHz) from the VICKSI heavy ion accelerator at the Hahn-Meitner-Institute in Berlin hits an iron-foil target (thickness 3 mg/cm^2, 90 % enriched in ^{57}Fe). More than 90 % of the excited ^{57}Fe recoils ejected from the target have angles between 15° and 75° with respect to the beam direction. These recoiling ions are trapped in a catcher made of the host material under investigation. The Mössbauer γ-radiation is detected in two resonance detectors of the parallel-plate-avalanche type (PPAC) with stainless-steel foil absorbers (53 % enriched in ^{57}Fe). A time resolution of 3 ns allows to measure the 14.4 keV Mössbauer radiation in a time window of about 380 ns between the beam bursts from the accelerator (AT 400 ns). This technique strongly reduces prompt background radiation. This set-up used for the experiments described in this section is shown in Fig. 6.16.

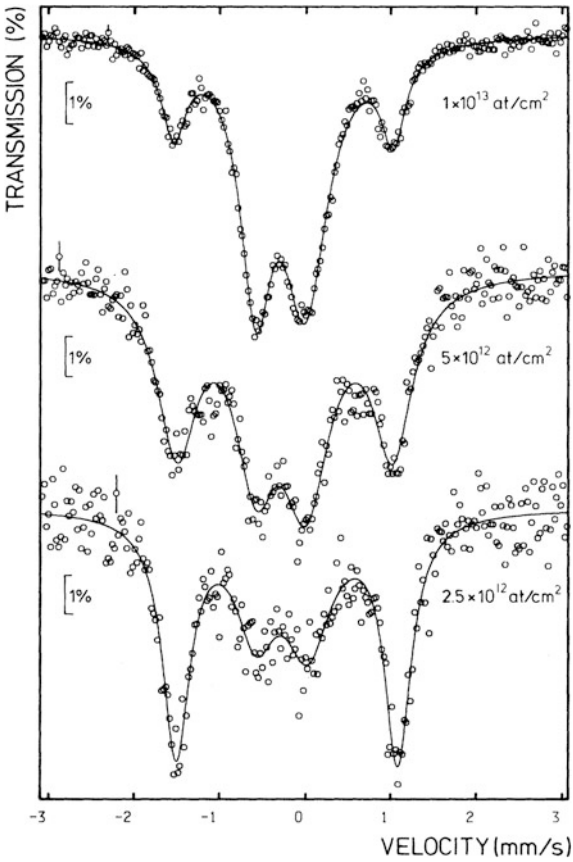

Fig. 6.14 Outer lines are assigned to Co_2 pairs in silicon [27]

6.3.2 *Fast Diffusion in Metals*

There are different diffusion mechanisms operating in materials, and their understanding is essential for solid state physics as well as for materials science. In many crystal systems such as pure iron and metallic alloys, self-diffusion and impurity diffusion proceed via vacancy mechanism, i.e., atomic jumps by exchanging an atom with a vacancy (A in Fig. 6.17), while light impurities such as hydrogen or carbon migrate via an interstitial mechanism, i.e., the impurities occupy interstitial sites and jump directly between the interstitial sites (B or C in Fig. 6.17). In the former system, the impurity diffusivities range in the same order of magnitude as the self-diffusivity, while in the latter systems, the impurity diffusivities are orders of magnitude higher than that of self-diffusivity.

There are, however, many systems showing anomalous fast diffusion, where metallic impurities such as Fe, Ni, Co, Cu, and Au in titanium, scandium, alkali, IVB group metals and semiconductors diffuse several orders of magnitudes faster than their self-diffusion in these materials, although the atomic sizes of the

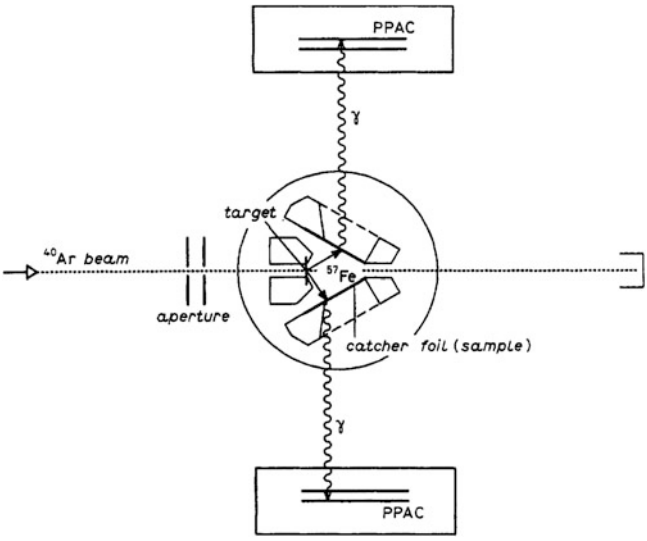

Fig. 6.15 Sketch of the experimental set-up for in-beam Mössbauer spectroscopy [29]

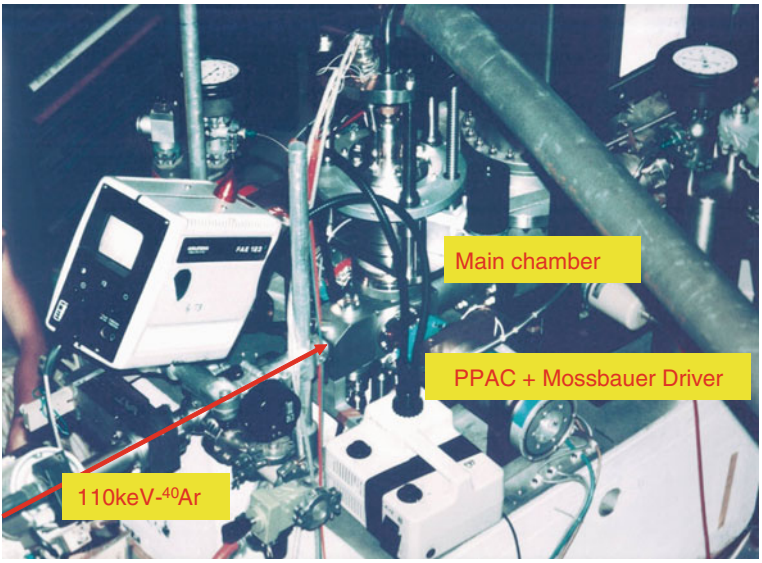

Fig. 6.16 The experimental set-up for in-beam Mössbauer spectroscopy at Hahn-Meitner Institute Berlin

impurities are comparable with those of the host atoms. This is amazing. If one thinks about the following situation, one can better understand how difficult to realize such fast diffusion: in rush-hour time, you, as an impurity, would be squeezed by your neighbors, the host atoms, in the middle of a crowded train, but

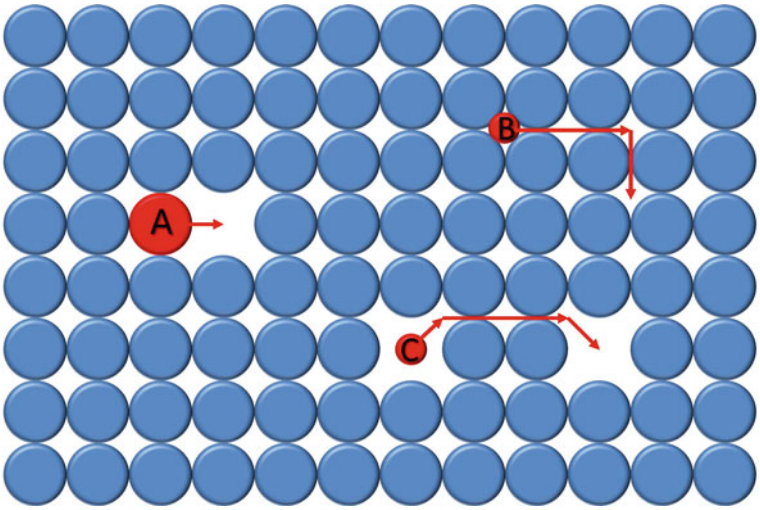

Fig. 6.17 Typical diffusion mechanism in solids

you would like to get out the train much faster than your neighbors. If you knew the mechanism of fast diffusion, you could quickly move through densely packed passengers.

One expects that some impurities occupy interstitial sites, leading to fast diffusion. However, it is rather difficult to understand how some metallic impurities could be incorporated into interstitial sites, when the atomic sizes of the impurities are taken into account. Hydrogen atoms could be easily put on interstitial sites in a crystal, but are not necessarily fast diffusers.

To clarify the origin of such anomalously fast diffusion, one must attempt a direct observation of the fast diffusing impurities by an experimental method. ^{57}Fe Mössbauer spectroscopy appears to be ideal, because it provides the atomistic information on the lattice sites, the charge states, the jump frequency and the jump vector, all of which are inevitably needed to construct an atomistic diffusion model. There were, however, two big problems to overcome experimentally: (1) the reliability of the available atomic jump theories in Mössbauer spectroscopy to deduce the jump parameters mentioned above from experimental spectra, and (2) the lack of Fe solubility which is generally reported in the fast diffusion systems. In order to realize isolated ^{57}Fe impurities in the samples mentioned in the former paragraph, the second problem appears to be impossible to solve as long as conventional absorber experiment are used. This is because neither a simple alloying, nor a low energy implantation of ^{57}Fe into a sample could provide an isolated ^{57}Fe atom without forming clusters of ^{57}Fe, which would mask the fast diffusing components in the Mössbauer spectrum.

To overcome the above mentioned difficulties in the studies of the fast diffusion in metals, several research projects were designed and performed in 1980s for about 10 years using the in-beam Mössbauer spectroscopy technique combining

Coulomb excitation with recoil implantation technique at the VICKSI accelerator facility in the Hahn-Meitner Institute Berlin.

6.3.3 Diffusion Study Using Mössbauer Spectroscopy

In the following sections we will show typical applications of in-beam Mössbauer spectroscopy for the study of fast diffusion in metals. Before getting into details, we are going to explain the principle of how the diffusion phenomenon affects the Mössbauer spectra. First of all, let us consider the following situation in our daily life: a fire engine sounding a siren is approaching you, while you are standing beside the street and are listening to the siren. The acoustic waves with a sound velocity of υ_s are emitted continuously during a time interval Δt from the fire engine moving at a velocity of υ_f. Consequently, the waves are compressed within a region of $(\upsilon_s - \upsilon_f)\cdot\Delta t$, leading to an observed sound frequency higher than that of the original frequency. This Doppler effect gives a possibility for us to get information on the motion by measuring the sound frequency even without watching directly the fire engine. More generally, when a matter is emitting a wave, a motion of matter changes the wave form. This will give you a hint to understand the principle of Mössbauer study on atomic jumps.

Now, in a solid matrix we have a Mössbauer probe of ^{57}Fe with a lifetime of 140 ns, as is shown in Fig. 6.18. The 14.4 keV first excited state of the ^{57}Fe nucleus can be fed through different processes, such as electron capture from ^{57}Co, β-decay from ^{57}Mn, Mössbauer absorption of 14.4 keV γ-ray, and Coulomb excitation. Subsequently the 14.4 keV γ-ray will be emitted resonantly without recoil (Mössbauer effect), while in Fig. 6.18, the ^{57}Fe atom is jumping between

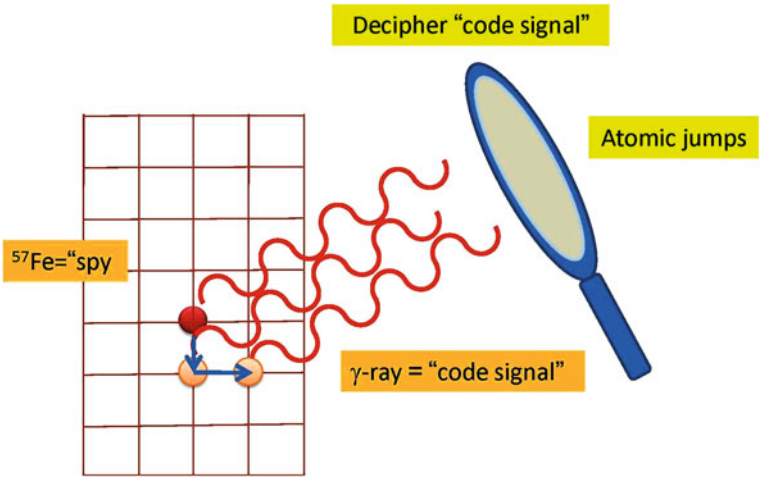

Fig. 6.18 Atomic motion influence on Mössbauer spectrum

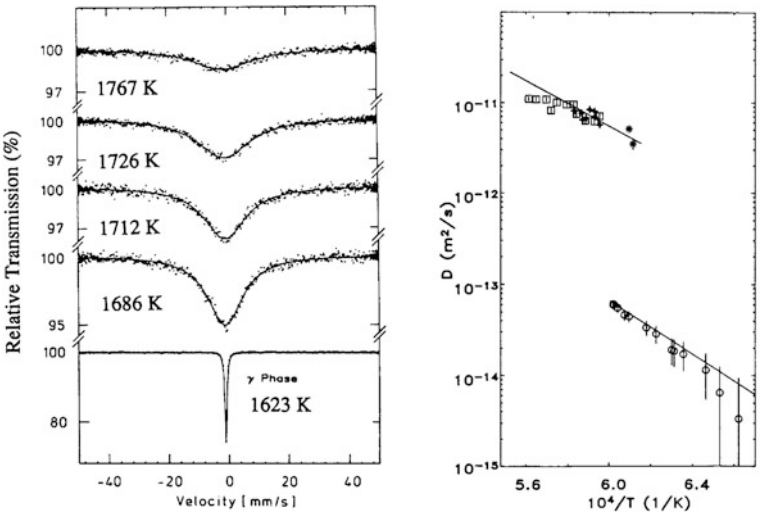

Fig. 6.19 Diffusional broadening of the Mössbauer resonance in Fe self-diffusion [30]

different lattice sites with a typical frequency of 10^7 s^{-1}, which is roughly equal to the inverse of the half-life time. In the crystal lattice, the atom is staying on the lattice positions, and is vibrating with a phonon frequency of 10^{12} s^{-1}. When the atom occasionally obtains thermal energy enough to overcome the potential barrier between the different lattice sites, the atom is able to jump from a lattice site to another, leading to diffusion. The duration of one jump is about 10^{-12} s, which is orders magnitude shorter than that of the atom staying on a lattice site. It turns out that the ^{57}Fe atom performs a few jumps during emitting or absorbing γ-ray, while the coherency of the wave is broken due to the jump process. Consequently, the lifetime of the 14.4 keV γ-ray is practically observed to be shorter than the natural lifetime. Taking into account of the Heisenberg time-energy uncertainty principle, $\Delta E \cdot \tau_M \approx h$, a shorter lifetime provides a broader linewidth of the Mössbauer resonance.

A typical example, that of a Mössbauer study of Fe self-diffusion [30], is shown in Fig. 6.19.

Iron has three different solid phases: the α-phase (bcc) up to 1,184 K, the γ-phase (fcc) up to 1,665 K, and the δ-phase (bcc) up to the melting point of 1809 K. The spectra of the γ- and δ-phases are shown in Fig. 6.19. The linewidths of all the spectra above 1656 K are much broader than that of the γ-phase spectrum at 1,623 K. The line broadenings observed in the δ-phase can be interpreted to be due to the atomic jumps of ^{57}Fe atoms within the lifetime, i.e. self-diffusion in the δ-phase. Since the line broadening, $\Delta\Gamma$, is related to the jump frequency, $1/\tau$, we can deduce the diffusion coefficient, D, using the following formula [30]:

$$D = \frac{R^2}{12\hbar} \cdot f(\theta) \cdot \Delta\Gamma$$

$$\Delta\Gamma = \frac{2\hbar}{\tau} \cdot \left[1 - \frac{1}{N} \sum_{n=1}^{N} \exp\left(i\vec{k} \cdot \vec{R}_n \right) \right]$$

Here R is a jump distance and $f(\theta)$ a correlation factor to take into account of the degree of the incoherency due to an angle, θ, between the jump vector, R_n and the wave vector of the 14.4 keV γ-ray, k. $f(\theta)$ depends both on crystal structures and on the diffusion mechanism, as discussed in [30].

Assuming a vacancy mechanism for the self-diffusion in γ- and δ-phases of pure Fe, the diffusivity was estimated from the line broadening using the above equation. The results are plotted as a function of 1/T in Fig. 6.19, in comparison with the tracer diffusivities for γ- and δ-phases, which were obtained by measuring the depth profiles of Fe tracers after annealing at different temperatures [30]. The diffusivities in both phases are in good agreement, indicating that the diffusion theory in Mössbauer spectroscopy can be applied even for studying an unknown diffusion mechanism such as fast impurity diffusion in metals.

6.3.4 In-beam Mössbauer Study on Fast Diffusion

The in-beam Mössbauer technique combining Coulomb-excitation and recoil-implantation, which was described in the Sect. 6.3.1, provides a unique feature for studying the anomalously fast diffusion, i.e., *one-by-one measurement*: Every γ-ray emission from ^{57m}Fe follows the implantation process. As a consequence, in the lattice the ^{57m}Fe probe always remains fully isolated from other ^{57}Fe atoms implanted before, and therefore, the spectrum obtained with this method is completely free from overlapping cascades as well as from clustering of Fe atoms. Both of them would change completely the diffusion properties of ^{57}Fe atoms. This method, therefore, guarantees an experimental condition under which we can follow a few jumps of ^{57m}Fe atoms immediately after the implantation into anomalously fast diffusion systems, such as α-Zr, Sc, and Pb.

Figure 6.20a–c show a typical spectra obtained from the In-beam Mössbauer experiments on ^{57}Fe in α-Zr [31, 32], Sc, and Pb [33], respectively. The spectra of ^{57}Fe in α-Zr (a) and Sc (b) consist mainly of a singlet and a doublet at the left and the right hand side, respectively, while the spectra of ^{57}Fe in Pb (c) appear to be only a singlet. First of all we discuss about the spectra of ^{57}Fe in α-Zr, which can be fitted with two different doublets. Their resonance areas, the quadrupole splittings of ΔEq, and the center shifts of δ are plotted as a function of temperature in Fig. 6.21a–c, respectively: (1) the electron density at ^{57}Fe nucleus, i.e., the isomer shift, is higher for the doublet than that of the singlet, and (2) the doublet shows dynamical behavior at around 50 K, which is observed as a quadrupole relaxation accompanied by a sudden decrease in the resonance area (Fig. 6.21a–c). These observations can be explained by the fast local jumps between equivalent

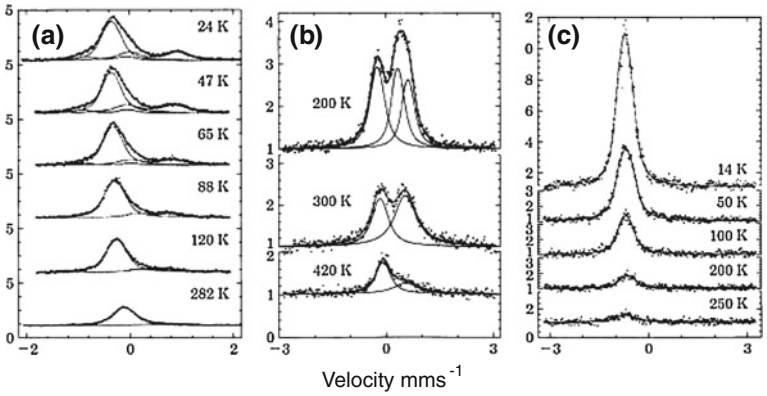

Fig. 6.20 In-beam Mössbauer spectra of ^{57}Fe in **a** α-Zr, **b** Sc, and **c** Pb

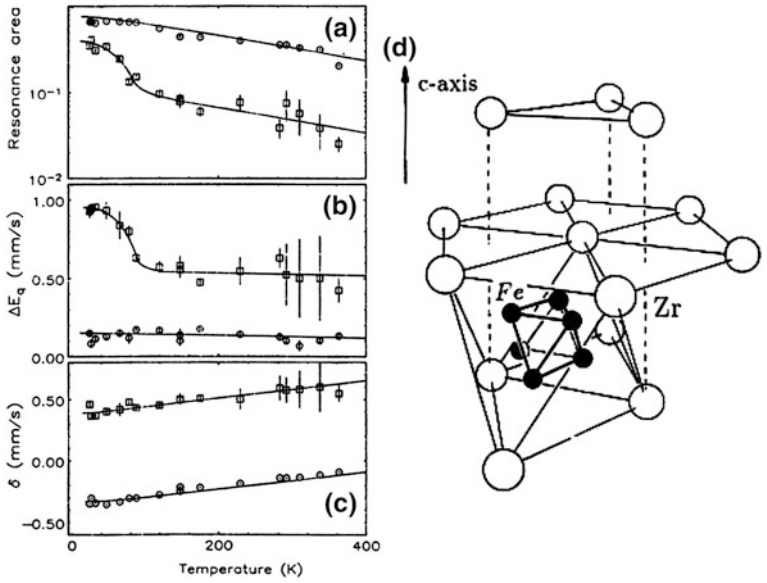

Fig. 6.21 Cage motion of Fe at interstitial equivalent positions. Fitting parameters for Mössbauer spectra of Fe in α-Zr as functions of temperature, and a possible model to explain the temperature dependence: **a** resonance areas, **b** quadrupole splitting ΔEq, and **c** center shifts δ [31]

"cage sites" as is shown in Fig. 6.21d. This cage motion is considered as a precursor to the long-range interstitial diffusion.

In the case of Sc in Fig. 6.20b, there seems to be a similar cage motion accompanied by both a quadrupole relaxation and a strong decrease of the area on the doublet at the right hand side at 300 and 450 K. In the case of Pb, on the other hand, the singlet shows a slight line broadening above 250 K, which could be due

to a fast long-range diffusion of Fe in Pb (Fig. 6.20c), but the effect was appeared to be too small to discuss into more details.

At the Hahn-Meitner Institute, in addition to the experiment on Fe in Si [26], as mentioned in the Sect. 6.2, Fe in alkaline metals was also studied using the same technique [33, 34].

6.4 On-line ^{57}Mn/^{57}Fe Implantation Mössbauer Spectroscopy at ISOLDE, CERN

The ISOLDE facility is a world-leading laboratory for the production and study of shortlived radioactive nuclei. ISOLDE belongs to CERN's accelerator complex situated on the border between Switzerland and France. The ISOLDE facility has been in operation since its start in 1967.

The radioactive nuclei are produced in reactions of high-energy protons from the PS-Booster accelerator in thick targets. The typical proton energies are between 1 and 1.4 GeV. More than 25 different target materials are used. The target material is kept at an elevated temperature so that the produced radioactive atoms diffuse out of the target into different dedicated ion sources. Ionisation can take place in a hot plasma, on a hot surface or by laser excitation. By judicious combinations of target-ions sources a chemical selectivity may be obtained and has resulted in selective production of more than 70 of the chemical elements. The ions are swept out of the ion-source by an applied voltage, accelerated to 30–60 kV and directed into an electro-magnet where they are separated according to their mass. In this way ISOLDE has been able to deliver more than 700 isotopically pure beams with intensities ranging from 1 to more than 10^{10} ions/s.

The main lines of research at ISOLDE are: nuclear structure physics, nuclear astrophysics, atomic physics, solid state physics, life sciences and fundamental interactions. A laboratory portrait been published as a special volume of Hyperfine Interactions [35]. In this volume a complete chapter is devoted to "Mössbauer Spectroscopy at ISOLDE" [36]. A schematic view of the set-up is shown in Fig. 6.22.

6.4.1 Site Selective Doping of III–V Semiconductors

The ^{119}Sn Mössbauer isotope can be studied in off-line emission Mössbauer experiments starting from the longlived ^{119m}Sn isomeric parent. The ISOLDE facility offers the interesting possibility to access the Mössbauer transition from the shortlived radioactive ^{119}In ($T_{1/2}$ = 2,3 min) and ^{119}Sb ($T_{1/2}$ = 38 h) precursor parents.

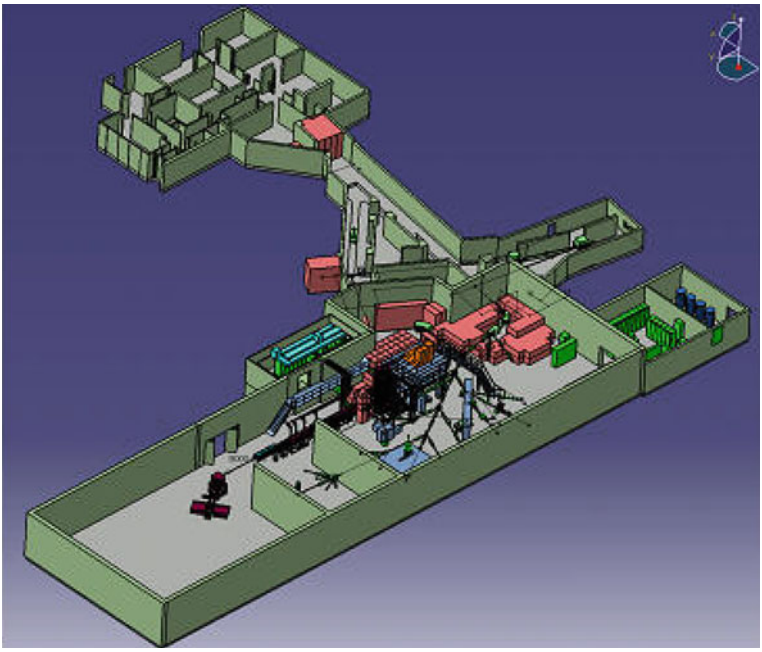

Fig. 6.22 ISOLDE lay-out

A very nice example of the power of Mössbauer spectroscopy was the demonstration [37] of site selective doping of compound III-V semiconductors such as GaAs, where it was concluded from the measured ^{119}Sn isomer shift that implanted In and Sb radioactive parent ions selectively populate III and V sites respectively.

6.4.2 Charge-State Dependent Diffusion of Fe in Si

As stated in the beginning of this tutorial, there are three different types of emission Mössbauer spectroscopy methods to study Fe in Si. They differ by the lifetime of the parent atom. We have first discussed in Sect. 6.2, the *off-line experiments* using the ^{57}Co radioactive parent with $T_{1/2} = 270$ d. We then mentioned in the Sect. 6.3 the *in-beam experiments* using the ^{57m}Fe parent with $T_{1/2} = 10^{-6}$ s. The third emission Mössbauer spectroscopy method makes use of a much shorter lived parent than ^{57}Co namely ^{57}Mn with a lifetime of $T_{1/2} = 1.5$ min. Two experimental facilities are nowadays making use of this method in *on-line experiments*: the ISOLDE facility at CERN and the RIKEN facility in Tokyo. These are huge experimental facilities to which access is granted through

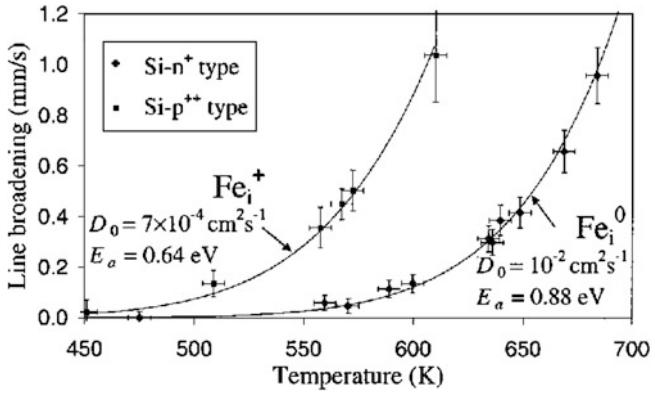

Fig. 6.23 Charge state dependent diffusivity of Fe in Si [38]

submission and approval of project proposals. In practice access for on-line ^{57}Mn experiments is limited to one week per year, at both experimental facilities. The authors of this tutorial are active at both sites.

The facilities are complementary in the energy of the ^{57}Mn beams provided. While the radioactive ^{57}Mn beams at CERN are accelerated to about 50 keV, as in the ^{57}Co off-line experiments discussed in Sect. 6.2, and result in shallow implantation depths of the order of 10 nm, the radioactive ^{57}Mn beams at RIKEN are accelerated to several 100 MeV resulting in implantation depths of hundreds of micrometers. As will be demonstrated in the Sect. 6.5, this allows to study materials deep below surface layers, as e.g. in electrode-covered solar cells.

Both on-line experimental facilities have been and are still involved in studies on Fe in Si. In the framework of this tutorial we show one such example [38]. The authors compared the Mössbauer spectra of ^{57}Fe in the decay of ^{57}Mn in two silicon samples with very different doping levels, extremely p-type (p^{++}) and highly n-type (n^{+}). They found that interstitial Fe atoms were created in silicon at 400–800 K as a result of the recoil imparted on these daughter atoms in the β-decay of ion-implanted, substitutional ^{57}Mn. Then they observed that diffusional jumps of the interstitial ^{57m}Fe cause a line broadening in their Mössbauer spectra, which is directly proportional to their diffusivity, as discussed in the preceding chapter. Thus, the charge-state-dependent diffusivity has been determined in differently doped material as shown in Fig. 6.23 [38].

6.5 On-line ^{57}Mn/^{57}Fe Implantation Mössbauer Studies at RIKEN

6.5.1 RIKEN RI Beam facility for On-line Mössbauer Spectroscopy

The Radioactive Ion Beam Factory (RIBF) accelerators will allow us to provide the world's most intense RI beams at energies of several hundreds MeV/nucleon over the whole range of atomic masses (Fig. 6.24). Recently, this facility has been upgraded by installing several heavy-ion accelerators on the bases of the former complex consisting of a K540 MeV ring cyclotron (RRC) and a couple of different types of the injectors: a variable-frequency heavy-ion linac (RILAC) and a K70 MeV AVF cyclotron (AVF). In the facility, a projectile-fragment separator (RIPS) provides the world's most intense light-atomic-mass (less than nearly 60)

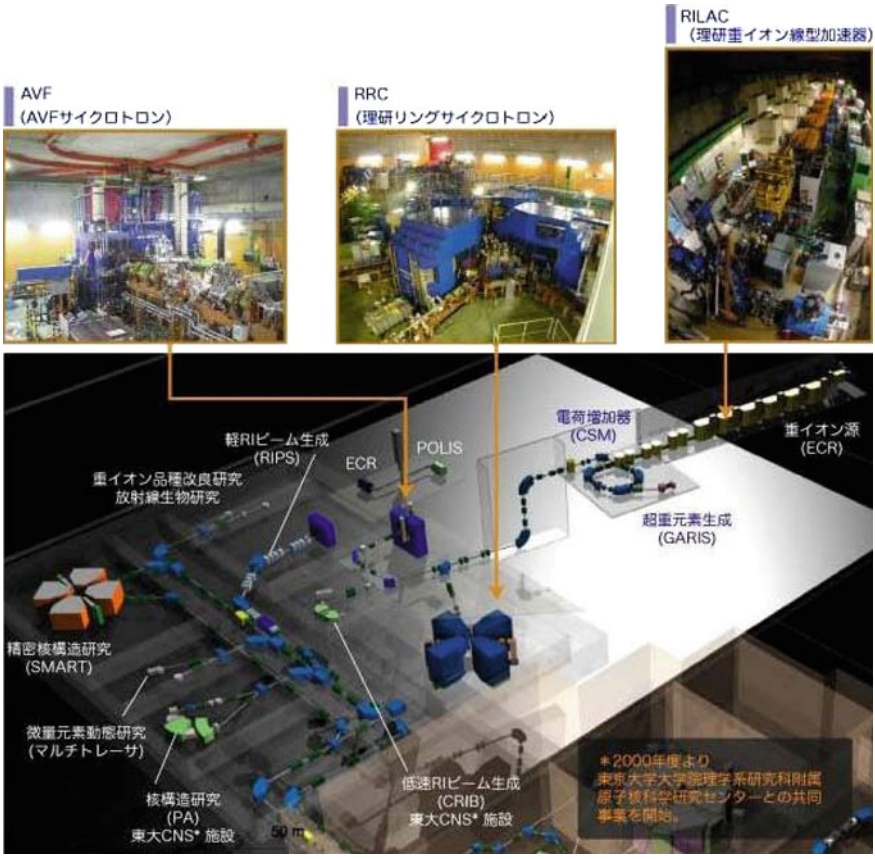

Fig. 6.24 RIKEN-RI beam facility

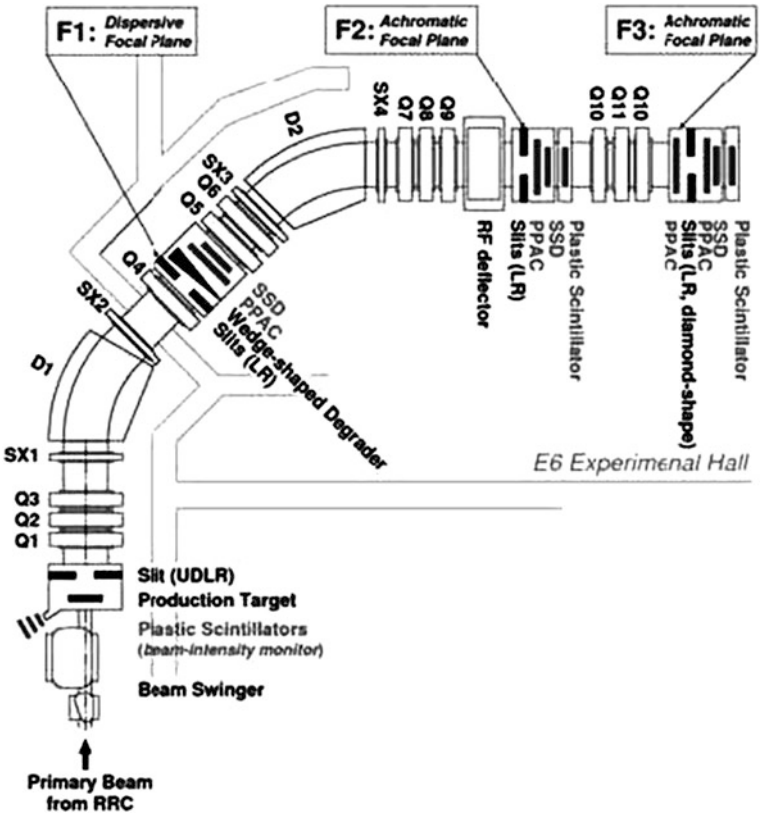

Fig. 6.25 RIKEN-separator configuration

RI beams. RIPS is an in-flight type radioactive isotope (RI) separator to produce RI beams using the fragmentation of the heavy ion beams. RIPS is an achromatic spectrometer, as is shown in Fig. 6.25, consisting of two magnetic separation sections, which enables us to separate RI beams with high resolution. For on-line Mössbauer spectroscopy, ^{57}Mn/^{57}Fe isotopes are separated by RIPS. The set-up for on-line Mössbauer spectroscopy of ^{57}Mn/^{57}Fe isotopes is installed at the end of the RIPS beam line behind the F3 chamber, as is shown in Fig. 6.26.

The on-line ^{57}Mn/^{57}Fe Mössbauer experiments were performed to clarify the lattice sites and the charge states of ^{57}Fe in Si materials at high temperatures up to 1,200 K [39–42] as well as under light illumination [43]. The implantation energy of ^{57}Mn/^{57}Fe used in this experiment is an order of GeV, which is several orders of magnitude higher than that used in other implantation experiments, and therefore the highest energy applied so far for solid state physics. At CERN, for instance, the energy is 60 keV. Generally speaking, a GeV-nuclear probe implanted into material is known to create a columnar defect due to the electrical stopping, and subsequently cascade damages due to the nuclear stopping interactions. At the last

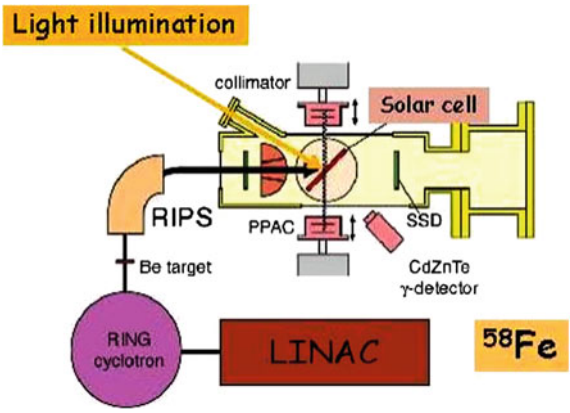

Fig. 6.26 Mössbauer set-up scheme at RIKEN

period of the landing processes, the nuclear probe will find different lattice sites close to this damage region either by landing directly on interstitial sites, or by substituting host atoms. In the case of ^{57}Mn implantation, the β-decay from ^{57}Mn to ^{57}Fe causes an additional small turbulence on the lattice sites of the probe, i.e., a recoil process of ^{57}Mn probe when emitting a highly energetic electron. The experimental results will tell us about the lattice sites as well as the charge states, as will be given in the followings.

Starting with a primary beam of ^{58}Fe, ^{57}Mn beam will be produced through the projectile fragmentation following a reaction with a Be target. Subsequently, the fragment of ^{57}Mn nuclei will be implanted into a sample, and will be stopped deeply in the matrix with an order of hundreds μm from the surface. The stopping range and their struggling, which are evaluated by TRIM code [9], are shown in Fig. 6.27 for the case of a Si crystal, and the result is compared with that of 100 keV-^{57}Fe implantation. Since the ion range of ^{57}Mn is 4 orders of magnitude higher than that of conventional low energy implantation, as described in the sections before, yielding us unique experimental conditions such as the low concentrations of ^{57}Mn as well as defects. One would speculate that GeV-implantation would produce only "amorphous", and therefore, no atomistic information could be studied through Mössbauer spectroscopy. The experimental results have, however, showed that we can send our "spy", i.e., ^{57}Mn/^{57}Fe deeply into the sample, and the spy send us, indeed, unique atomistic information on the nuclear probes and their surrounding lattice in Si materials.

6.5.2 ^{57}Mn/^{57}Fe Experiments on Si

As stated before, iron impurities in Si have been intensively investigated for more than 50 years by different experimental techniques [44] including ^{57}Fe Mössbauer spectroscopy. This is because Fe impurities can be easily incorporated into Si

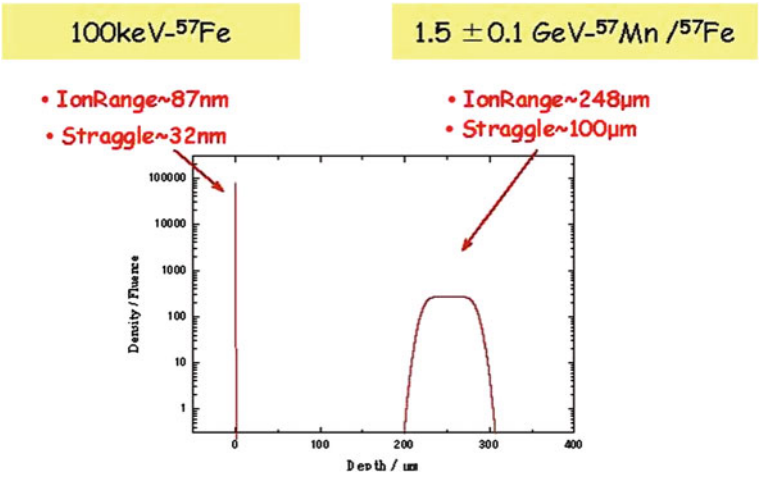

Fig. 6.27 Ion ranges of ^{57}Mn/^{57}Fe at RIKEN compared with conventional separator

matrix during the industrial processes, causing serious degradation in the electronic properties of silicon-based devices and also solar cells on one hand. Atomistic information on Fe impurities in Si, on the other hand, is essential to understand dynamical properties such as atomic diffusion as well as carrier transport. Fe impurities are known to form the deep levels in the Si band gap, producing strong trapping centres for the carriers in the devices: Interstitial Fe_i are well known to form a donor level at 0.39 eV from the valence band edge, while substitutional Fe_s is expected to form an accepter level of 0.69 eV from the first principle calculation [45]. Although interstitial and substitutional Fe have been detected as spectral components in ^{57}Fe Mössbauer experiments, the charge states could not be well distinguished experimentally so far in terms of isomer shifts.

Typical Mössbauer spectra of ^{57}Fe in n-type FZ-Si in the temperature region between 330 K and 1,200 K are shown in Fig. 6.28. The spectra from 300 to 700 K can be fitted by two singlets of Lorentzians, while the spectra from 800 up to 1,200 K can be analyzed only by a broad singlet. The two singlets at 330 K at the left and the right hand site have been assigned to ^{57}Fe atoms on interstitial and substitutional sites in Si matrix, respectively. This assignment is based on a theoretical calculation of the isomer shifts [46], which relate with the charge density at ^{57}Fe nucleus. The spectra and their fitting parameters are changing anomalously with elevating temperature. These behaviors are in good agreement with the former experiments on p-type FZ-Si wafers up to 800 K [39–41]. The resonance area of the interstitial ^{57}Fe component at the left hand side decreases strongly above 500 K.

A "peak position of a component" in the Doppler velocity scale provides us information both on the different lattice sites of ^{57}Fe atoms and their charge states. This shift is called "center shift", depending on the isomer shift and the second-order Doppler (SOD) shift. As a reference, the broken line in Fig. 6.28 shows the

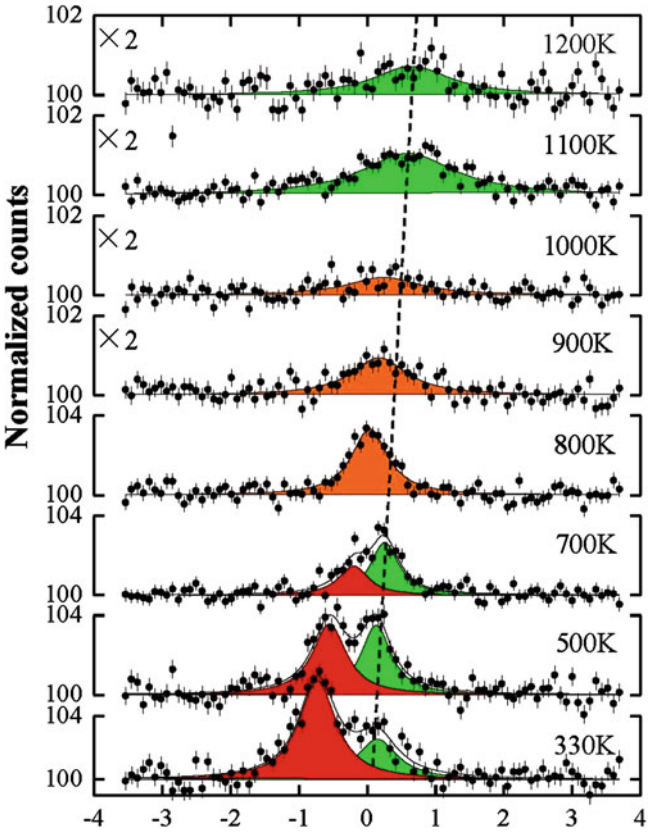

Fig. 6.28 Mössbauer spectra of ^{57}Fe in n-type FZ-Si measured between 330 and 1,200 K. Notice that the vertical scale for the region above 900 K is blown up with a factor of two, in order to show the small and broad resonance effects more clearly [42]

usual temperature dependence of a spectrum component due to the SOD shift. Both the interstitial and the substitutional components, however, do not simply follow the SOD shift. The center shift of the interstitial component deviates from the SOD shift, moving continuously to the substitutional position with increasing temperature. This anomaly is accompanied by the strong decrease of the resonance area. Furthermore, the center shifts of the substitutional singlet between 800 and 1,000 K are different from the extrapolation of the center shift, but above 1,100 K the shift goes back to the position of the substitutional again. This is essential observation to interpret the whole dynamical phenomena (Fig. 6.29).

Above 500 K interstitial Fe atoms are supposed to start migrating within the lifetime, subsequently finding vacancies. Consequently, the singlet between 800 and 1,000 K is thought to be a "motional-averaged component" due to substitutional ^{57}Fe formation. Above 1,100 K the isomer shift of the broad singlet coincides with that of substitutional Fe, indicating that Fe atoms stay dominantly on

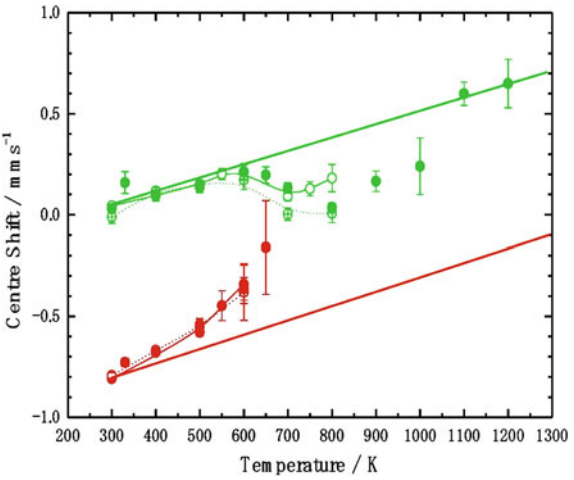

Fig. 6.29 Line positions in the spectra of Fig. 6.28

substitutional sites, jumping via vacancies. The theoretical treatment [42] is, however, beyond this tutorial level.

6.5.3 ^{57}Mn/^{57}Fe Experiments on Si Solar-Cells

Multi-crystalline silicon is widely used for solar cells, but contains different lattice defects and metallic impurities such as iron atoms, which produce carrier trapping centers, and therefore, degrade the energy conversion efficiency of solar cells. No direct observation on the charge states of Fe atoms has been achieved in multi-crystalline Si solar cells during operation, i.e. under light illumination. The Fermi Level will be shifted by injecting the excess carriers, and consequently different charge states of interstitial and substitutional Fe atoms are expected to appear in the on-line Mössbauer spectra of ^{57}Mn/^{57}Fe in mc-Si under light illumination [43]. Figure 6.30 shows the top and the back surfaces of mc-Si solar cell. Ag electrodes on an anti-reflection Si–N layer can be seen and the ^{57}Mn implantation was performed through this top surface. During a Mössbauer spectral measurement under dark condition, I–V characteristic of the p-n junction was measured every one hour, in order to control the defect accumulation due to ^{57}Mn implantation. The I–V curve, however, did not change with increasing the implantation dose of ^{57}Mn.

The spectrum of ^{57}Mn/^{57}Fe in the p-region of the p-n junction, i.e., solar cell, was measured at 400 K under light illumination. In Fig. 6.31a this spectrum (red points) was compared with that in p-type multi-crystalline (mc)-Si (Black points). The "black spectrum" consists of two components, as is shown with red and green components in Fig. 6.31a. They are assigned to interstitial and substitutional Fe in Si matrix with the isomer shifts of 0.8 and -0.06 mms^{-1}, respectively. On the other hand, the "red spectrum" of the solar cell is very broad, and therefore, is

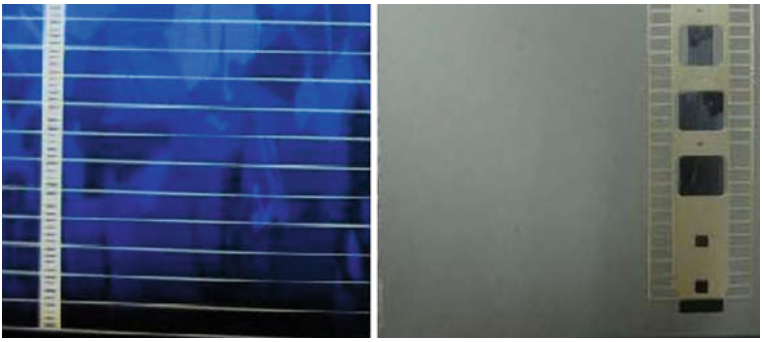

Fig. 6.30 Top and back surfaces of a silicon solar cell (30 × 30 mm in square) which was specially provided by Kyocera

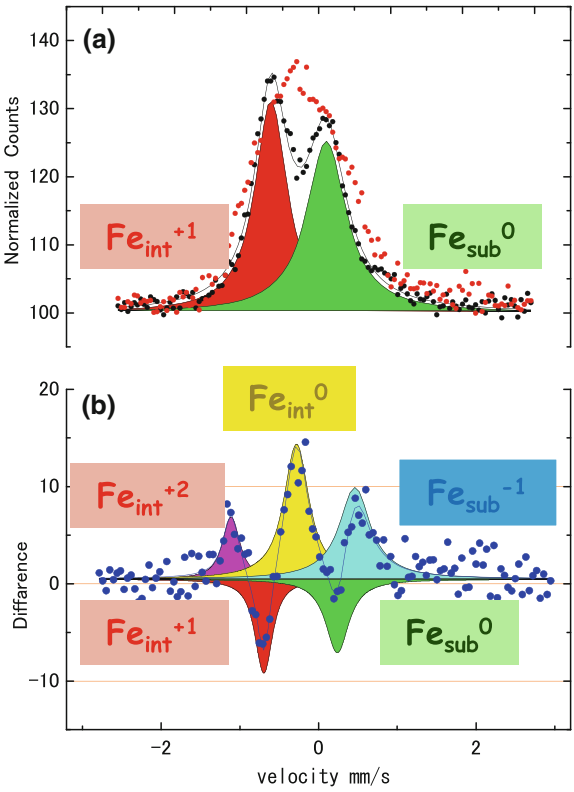

Fig. 6.31 **a** Mössbauer spectrum of ^{57}Mn/^{57}Fe in p-type multi-crystalline-Si (*black points*) is compared with that in Si-solar cells (*red points*) at 400 K under Xe lamp illumination. The *black spectrum* is fitted with *red* and *green* components. **b** The difference of the *red* and *black spectra* is shown with blue points. The difference spectrum can be analyzed by the appearing *three* singlets (*pink*, *yellow*, and *light blue* components and the *two* disappearing singlets (*red* and *green* components)

difficult to analyze by a superposition of singlets. To interpret such broad spectrum, we subtract the "black spectrum" from the "red spectrum". The difference spectrum (blue points) in Fig. 6.31b can be fitted by three appearing components (pink, yellow, and light blue) and two disappearing ones (red and green).

These singlets are considered to correspond to different charge states of interstitial Fe_i and substitutional Fe_s: Fe_i^{2+}, Fe_i^{1+}, Fe_i^0, Fe_s^0, and Fe_s^{-1} are colored by pink, red, yellow, green and light blue, respectively in Fig. 6.31b. The isomer shift values are in good agreement with those of previous absorber experiments obtained in ^{57}Fe-diffused mc-Si [47]. Notice that the ^{57}Mn probes were implanted into the p-type region of mc-Si solar cell, which is the same material as the p-type mc-Si wafer. The present results indicate that the light illumination changes not only in the Fermi level (quasi-Fermi level) by the excess carrier injection, but also in the carrier trapping processes. The latter must be due to the directional excess carrier flow through the p-n junction, which affects the carrier trapping kinetics with electrons and holes at the Fe impurities, leading to the different charge states on both Fe substitutional and interstitial sites in the p-region in mc-Si solar cell. This is, in fact, the first in situ observation of the carrier trapping processes at Fe impurities in mc-Si solar cell, which degrades the energy conversion efficiency.

6.6 Conclusions

In this tutorial we have attempted to explain the principles of ion implantation and of the dedicated Mössbauer techniques that were developed to perform off-line, in-beam and on-line emission Mössbauer spectroscopy after implantation of radioactive probe atoms.

We have illustrated these principles with numerous examples, focusing on Fe in Si, which can be studied by all three techniques.

We hope to have demonstrated the enormous resolving power on atomistic scale of emission Mössbauer spectroscopy for such studies. For Fe impurities in Si, with their extremely complex behavior, these techniques have clearly shown their merits and have substantially contributed to our understanding of the behavior of Fe impurities in Si.

References

1. E.L. Wolf, *Nanophysics and Nanotechnology*: *An Introduction to Modern Concepts in Nanoscience* (Wiley-VCH, New York, 2006)
2. Electron Microscope
3. C. Kittel, *Introduction to Solid State Physics*, 8th edn. (Wiley, New York, 2005
4. R.L. Mössbauer, Z. Physik, **151**, 124 (1958)
5. R.L. Mössbauer, Naturwissenschaften, **45**, 538 (1958)
6. R.L. Mössbauer, Z. Naturforsch. **14a**, 211 (1959)
7. Hyperfine Interactions
8. L.C. Feldman, J.W. Mayer (eds.), *Fundamentals of Surface and Thin Film Analysis*. (Appleton and Lange, New York, 1986)
9. J.F. Ziegler, J.P. Biersack, U. Littmark, *The Stopping and Range of Ions in Solids* ed. (Pergamon Press, New York, 1985); http://www.srim.org/

10. G. Langouche, *Hyperfine Interaction of Defects in Semiconductors* (Elsevier, Amsterdam, 1992)
11. G. Langouche, in *Mössbauer Spectroscopy Applied to Inorganic Chemistry*, G. Long, F. Grandjean (eds.), Vol. 3, (Plenum Press, New York and London, 1989), pp. 445–512
12. H. de Waard, S.A. Drentje, Phys. Lett. **20**, 38 (1966)
13. G.L. Latshaw, Stanford University, PhD Thesis, 1971
14. L. Niesen, Hyperfine interact. **13**, 65–88 (1983)
15. G. Weyer, Hyperfine Interact. **27**, 249–262 (1986)
16. H. de Waard, Hyperfine Interact. **40**, 31–48 (1988)
17. G. Langouche, Hyperfine Interact. **45**, 199–216 (1989)
18. G. Langouche, Hyperfine Interact. **72**, 217–228 (1992)
19. M. de Coster, H. Pollak, S. Amelinckx, in *Proceedings of the 2nd International Conference on the Mössbauer Effect,* D.M.J. Compton, A.H. Schoen (eds.) (Wiley, New York, 1962), p. 289
20. P.C. Norem, G.K. Wertheim, J. Phys. Chem. Solids **23**, 1111 (1962)
21. G. Langouche, M. de Potter, I. Dézsi, M. Van Rossum, Radiat. Effect Lett. **67**, 404 (1982)
22. J.A. Sawicki, B.D. Sawicka, Phys. Stat. Sol. b **86**, K159 (1978)
23. G.L. Latshaw, P.B. Russell, S.S. Hanna, Hyperfine Interact. **8**, 105–127 (1980)
24. J.A. Sawicka, B.D., Sawicki, J.A. Phys. Lett. A **64**, 311 (1977)
25. G. Langouche, M. de Potter, Nucl. Instrum. Methods B **19/20**, 322 (1987)
26. P. Schwalbach, S. Laubach, M. Hartick, E. Kankeleit, B. Keck, M. Menningen, R. Sielemann, Phys. Rev. Lett. **64**, 1274 (1990)
27. G. Langouche, M. de Potter, D. Schroyen, Phys. Rev. Lett. **53**, 1364 (1984)
28. W. Bergholz, Physica B **16**, 312 (1983)
29. M. Menningen, R. Sieleman, G. Vogl, Y. Yoshida, K. Bonde-Nielsen, G. Weyer, Europhys. Lett. **3**, 927–933 (1987)
30. A. Heiming, K.H. Steinmetzt, G. Vogl, Y. Yoshida, J. Phys. F: Met. Phys. **18**, 1491–1503 (1988)
31. Y. Yoshida, M. Menningen, R. Sielemann, G. Vogl, G. Weyer, K. Schroeder, Phys. Rev. Lett. **61**, 195 (1988)
32. Y. Yoshida, Hyperfine Interact. **47**, 95–113 (1989)
33. R. Sielemann, Y. Yoshida, Hyperfine Interact. **68**, 119–130 (1991)
34. B. Keck, R.Sielemann, Y. Yoshida, Phys. Rev.Lett.
35. D. Forkel-Wirth, ISOLDE laboratory portrait. Hyperfine Interact. **129** (2000)
36. G. Weyer, Hyperfine Interact. **129**, 371–390 (2000)
37. G. Weyer, J.W. Petersen, S. Damgaard, H.L. Nielsen, Phys. Rev. Lett. **44**, 155–157 (1980)
38. H.P. Gunnlaugsson, G. Weyer, M. Dietrich and the ISOLDE collaboration, M. Fanciulli, K. Bharuth-Ram, R. Sielemann, Appl. Phys. Lett. **80**, 2657–2659 (2002)
39. Y. Kobayashi, Y. Yoshida et al., Hyperfine Interact. **126**, 417 (2000)
40. Y. Yoshida, K. Kobayashi et al., Defect Diffus. Forum **194–199**, 611 (2001)
41. Y. Yoshida; ALTECH 2003 Analytical and Diagnostic Techniques for Semiconductor Materials, Devices, and Processes, 479 (2003)
42. Y. Yoshida, Y. Kobayashi, K. Hayakawa, K. Yukihira, A. Yoshida, H. Ueno, F. Shimura, F. Ambe; Physica B, **376-377**, 69 (2006)
43. Y. Yoshida, K. Suzuki, Y. Kobayashi, T. Nagatomo, Y. Akiyama, K. Yukihira, K. Hayakawa, H. Ueno, A. Yoshimi, D. Nagae, K. Asahi, G. Langouche, Hyperfine Interact. **204**, 133–137 (2012)
44. A.A. Istratov, H. Hieslmair and E. R. Weber; Appl. Phys. A **69**, 13 (1999)
45. S. K. Estreicher, M. Sanati, N. Gonzalez Szawacki, Phys. Rev. B, **77**, 125214 (2008)
46. J. Kübler, A. E. Kumm, H. Overhof, P. Schwalbach, M. Hartick, E. Kankeleit, B. Keck, L.Wende, R.Sielemann, Z. Phys., B **92**, 155 (1993)
47. Y. Yoshida, S. Horie, K. Niira, K. Fukui and K. Shirasawa; Physica B, **376–377**, 227 (2006)
48. T. Diaz de la Rubia and G. H. ilmer, Phys. Rev.Lett., **74**, 2507-2510 (1995)

Author Biographies

Guido Langouche

Since 2010 Guido Langouche is emeritus professor in nuclear solid state physics at the University of Leuven. After obtaining his doctoral and habilitation degrees from K.U.Leuven, he was post-doc at the universities of Stanford and Groningen and guest professor at the universities of Osaka, Lyon and Kinshasa.

From 1995 till 2005 he was vice-rector of K.U.Leuven.

From 2005 till 2010 he was chairman of the Coimbra Group, an academic collaboration network of 40 of Europe's longest-established research-intensive universities.

He is presently vice-president of NVAO, the *Accreditation Agency for the Netherlands and Flanders*, residing in The Hague, where he was appointed in 2007 jointly by the Dutch and Flemish Ministers of Education.

Since 2011 he is also Secretary of INQAAHE, the *International Network for Quality Assurance Agencies in Higher Education*.

He is editor-in-chief of the *Hyperfine Interactions* journal.

Representative publication

1. G. Langouche "Hyperfine interactions of defects in semiconductors" Elsevier 1992, 489 pages.
2. G. Langouche "Characterization of semiconductors by Mössbauer Spectroscopy" in "Mössbauer Spectroscopy applied to inorganic chemistry – Volume 2" p 445-512, editors G. Long and F. Grandjean, Plenum Press, New York 1989.
3. G. Langouche "Ion implantation in semiconductors studied by Mössbauer Spectroscopy", Hyperfine Interactions 45 (1989) 199–216.
4. G. Langouche "Ion implantation" Hyperfine Interactions 68 (1991) 95–106.

Yutaka Yoshida

Since 2004 Yutaka Yoshida is professor in Materials and Life Science at Shizuoka Institute of Science and Technology, Japan, following associate professor at the same institute between 1991 and 2003. After obtaining his doctoral degree from Osaka University under the guidance of emeritus Professor F.E. Fujita, and he stayed in the group of Professor Gero Vogl as a guest scientist at the Hahn-Meitner Institute Berlin, Germany, in the period between 1983 and 1985, and 1990, and also as a research assistant at the Institute of solid state physics, Universität Wien, Austria, between 1986 and 1989.

Since 1993 he is a guest Scientist at the RIKEN, Japan. He is the chairperson of ICAME 2011 at Kobe.

Representative publication:

1. Y. Yoshida; “In-Beam Mössbauer Study of Atomic Jump Processes in Metals”, Hyperfine Interactions, 47, 95-113 (1989).
2. Y. Yoshida and F. Shimura, “In-Situ Observation of Diffusion and Segregation of Fe atoms in Si Crystals at High Temperature by Mössbauer spectroscopy”, in Electrochemical Society Proceedings, 98-1, 984-996 (1998).
3. Y. Yoshida, “Mössbauer spectroscopy to investigate atomistic jump processes on an atomistic scale”, Hyperfine Interactions, 113, 183-198 (1998).
4. Y. Yoshida, “Direct Observation of Substitutional and Interstitial Fe atoms in Si by high-temperature and In-beam Mossbauer Spectroscopy”, in ALTECH 2003, ECS, Salt Lake City, US, 479-482 (2003).